JACS
JOURNAL OF THE AMERICAN CHEMICAL SOCIETY

COMMUNICATION

pubs.acs.org/JACS

A Manganese(V)−Oxo π-Cation Radical Complex: Influence of One-Electron Oxidation on Oxygen-Atom Transfer

Katharine A. Prokop,[†] Heather M. Neu,[†] Sam P. de Visser,[*,‡] and David P. Goldberg[*,†]

[†]Department of Chemistry, The Johns Hopkins University, Baltimore, Maryland 21218, United States

[‡]Manchester Interdisciplinary Biocentre and School of Chemical Engineering and Analytical Science, University of Manchester, 131 Princess Street, Manchester M1 7DN, U.K.

Supporting Information

ABSTRACT: One-electron oxidation of Mn^{V}−oxo corrolazine **2** affords $\mathbf{2}^{+}$, the first example of a $Mn^{V}(O)$ π-cation radical porphyrinoid complex, which was characterized by UV−vis, EPR, LDI-MS, and DFT methods. Access to **2** and $\mathbf{2}^{+}$ allowed for a direct comparison of their reactivities in oxygen-atom transfer (OAT) reactions. Both complexes are capable of OAT to PPh_3 and RSR substrates, and $\mathbf{2}^{+}$ was found to be a more potent oxidant than **2**. Analysis of rate constants and activation parameters, together with DFT calculations, points to a concerted OAT mechanism for $\mathbf{2}^{+}$ and **2** and indicates that the greater electrophilicity of $\mathbf{2}^{+}$ likely plays a dominant role in enhancing its reactivity. These results are relevant to comparisons between Compound I and Compound II in heme enzymes.

A wide range of heme (e.g., cytochrome P450s, peroxidases)[1] and non-heme metalloenzymes,[2] as well as biomimetic synthetic catalysts,[3] mediate the oxidation of organic substrates via proposed high-valent iron−oxo and manganese−oxo intermediates. Fundamental recurring processes in these oxidation reactions include hydrogen-atom transfer (HAT) and oxygen-atom transfer (OAT) to/from the metal−oxo unit. High-valent Mn(O) species have also been implicated in photosynthetic water splitting, in which the critical O−O bond may be formed by nucleophilic attack of H_2O/OH^{-} on an electrophilic Mn(O) unit,[4] a process reminiscent of OAT with H_2O as the "organic" substrate. Thus, there is great interest in delineating the structural and electronic properties of high-valent Fe(O) and Mn(O) complexes, and a key challenge is to determine what factors are crucial for controlling their reactivity.[5] However, the direct observation of these metal−oxo species is difficult because of their inherent instability. For example, manganese(III) porphyrins are powerful catalysts for OAT processes, but the direct examination of high-valent $Mn^{V}(O)$ porphyrins is rare.[6]

Significant efforts have been made to determine the relative reactivities of iron(IV)−oxo porphyrin$^{+\bullet}$, designated as Compound I (Cpd-I), versus iron(IV)−oxo porphyrin (Cpd-II), for both heme enzymes and model complexes.[5c,7] To our knowledge, however, there have been no reports of a direct comparison of the reactivities of a similar pair of Mn(O)(porphyrin$^{+\bullet}$)/Mn(O)(porphyrin) complexes, most likely because of a lack of access to such species.[8] Corrolazines, along with their corrole analogues, impart special stability to high-valent metal ions that distinguishes them from their porphyrin congeners.

Scheme 1. One-Electron Oxidation of $(TBP_8Cz)Mn^{V}(O)$

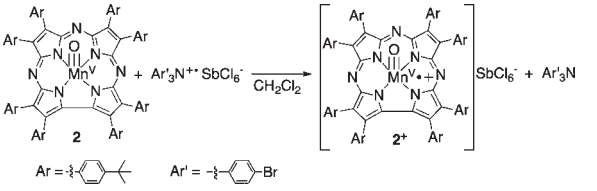

We previously showed that oxidation of the Mn^{III} corrolazine $(TBP_8Cz)Mn^{III}$ (**1**) [TBP_8Cz = octakis(*p-tert*-butylphenyl)-corrolazinato^{3-}] gave the isolable Mn^{V}−oxo complex $(TBP_8Cz)Mn^{V}(O)$ (**2**).[9] Despite the stability of **2**, it is capable of both HAT and OAT oxidation reactions.[9a,c,d]

Herein we report the oxidation of the neutral $Mn^{V}(O)$ complex **2** to afford the one-electron-oxidized complex $[(TBP_8Cz)Mn(O)]^{+}$ ($\mathbf{2}^{+}$) (Scheme 1). Spectroscopic analyses and density functional theory (DFT) calculations have shown that this complex is best described as a $Mn^{V}(O)$ corrolazine π-cation radical $[(TBP_8Cz^{+\bullet})Mn^{V}(O)]$, the first example of a $Mn^{V}(O)$ π-cation radical species. Access to **2** and $\mathbf{2}^{+}$ has made possible a comparison of the reactivities of two high-valent Mn(O) complexes that differ in the same manner as Cpd-I and Cpd-II. We have determined the OAT reactivities of **2** and $\mathbf{2}^{+}$ with thioether substrates, providing a direct measure of the influence of the change in oxidation level on OAT reactions. The results of kinetic measurements and DFT calculations are in excellent agreement with each other and provide a mechanistic framework that addresses the origins of this influence.

Previously, cyclic voltammetry (CV) measurements on **2** in CH_2Cl_2 or PhCN revealed a reversible reduction near 0.0 V vs SCE that was assigned to the metal-centered Mn^{V}/Mn^{IV} couple.[9b] Complex **2** also showed two well-separated oxidations, the first appearing as a reversible wave centered at 1.02 (1.09) V in CH_2Cl_2 (PhCN) and the second as an irreversible oxidation at E_{pa} = 1.57 (1.52) V.[9b] Time-resolved thin-layer UV−vis spectra for the controlled-potential oxidation of **2** at 1.20 V in PhCN revealed a decrease and blue shift of the Soret band at 425 nm, a decrease of the Q band at 633 nm, and an increase in a broad shoulder at 718 nm. These spectral changes suggested a corrolazine-ring-centered oxidation, although metal-centered oxidation to give a Mn^{VI} complex could not be ruled out. To gain further insight into the locus of oxidation and potentially

Received: July 15, 2011
Published: September 02, 2011

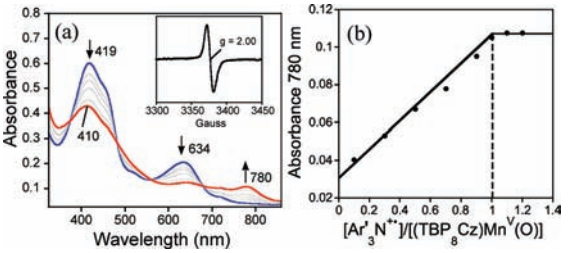

Figure 1. (a) UV−vis spectra of the oxidation of **2** (10 μM) with increasing amounts of $[Ar'_3N^{+\bullet}](SbCl_6^-)$ (0−1.2 equiv) at 25 °C in CH_2Cl_2. Inset: X-band EPR spectrum of $\mathbf{2}^+$ (10 μM) at 15 K in CH_2Cl_2. (b) Spectral titration to determine the stoichiometry of the reaction.

access a novel Mn−oxo complex at the formal Mn^{VI} oxidation level, we targeted the bulk production of this species via chemical oxidation.

Reaction of **2** (10 μM) with 1 equiv of the one-electron oxidant $[Ar'_3N^{+\bullet}](SbCl_6^-)$ (Ar′ = 4-BrC_6H_4; E_{ox} = 1.16 V vs SCE)[10] in CH_2Cl_2 at 25 °C (Scheme 1) led to the immediate isosbestic conversion of bright-green **2** to an orange-brown solution with new peaks at λ_{max} = 410 and 780 nm (Figure 1a). The decrease in the Soret and Q bands of **2** along with the appearance of a band at longer wavelength (780 nm) is similar to the transformation seen upon controlled-potential oxidation of **2** in PhCN[9b] and analogous corrole oxidations.[11] Oxidation of **2** could also be accomplished with cerium(IV) ammonium nitrate (CAN), as shown by UV−vis spectra when 1 equiv of CAN dissolved in ∼100 μL of CH_3CN was added to **2** in CH_2Cl_2 (2 mL) [Figure S3 in the Supporting Information (SI)]. A spectral titration with $[Ar'_3N^{+\bullet}]$ (Figure 1b) confirmed the 1:1 stoichiometry for the electron-transfer process and indicated the formation of a one-electron-oxidized product, $[(Cz)Mn(O)]^+$.

Orange-brown $\mathbf{2}^+$ is stable in dilute solution for over 24 h, but significant decomposition occurs upon concentration to dryness. Despite this relative instability, laser desorption ionization mass spectrometry (LDI-MS) on samples of $\mathbf{2}^+$ deposited and evaporated rapidly on the LDI-MS target plate gave rise to a prominent isotopic cluster centered at m/z 1426.8 in positive-ion mode (Figure S1). This cluster matches the expected theoretical isotope distribution for $\mathbf{2}^+$. Exchange of the terminal oxo group in **2** with $H_2{}^{18}O$ gave the ^{18}O isotopomer (**2-^{18}O**) with high isotopic enrichment (97% ^{18}O), as previously reported.[9a] One-electron oxidation of this material resulted in a shift of the isotopic cluster consistent with partial retention of the ^{18}O label (60% ^{18}O) (Figure S2). It is likely that some scrambling occurred with residual H_2O originating from the solvent or from the oxidant in this case (CAN). These data confirmed the formulation of $\mathbf{2}^+$ as $[(Cz)Mn(O)]^+$.

The electron paramagnetic resonance (EPR) spectrum of $\mathbf{2}^+$ at 15 K in CH_2Cl_2 shows a sharp singlet at g = 2.001 (line width = 15 G) with no hyperfine splitting from the Mn ion (Figure 1a inset). The signal was quantified against an external standard, revealing a 77% yield of $\mathbf{2}^+$. The data suggest that the ground state retains a low-spin d^2 configuration for the Mn^V ion, as seen in the neutral starting material, with oxidation resulting in a π-cation radical on the corrolazine ring. Furthermore, the lack of hyperfine splitting from N atoms suggests that the spin density is concentrated on the pyrrole carbon atoms. The same EPR spectrum was observed irrespective of the oxidant employed (CAN or $[Ar'_3N^{+\bullet}]$). The EPR spectrum of $\mathbf{2}^+$ is similar to that observed for metallocorrole π-cation radicals.[11,12]

To model the electronic structure of $\mathbf{2}^+$, DFT calculations at the B3LYP level were performed as described previously.[13] Full

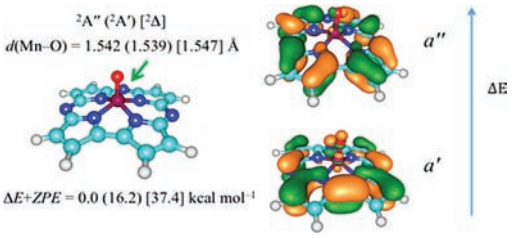

Figure 2. DFT-calculated optimized geometries of the $^2A'$, $^2A''$, and $^2\Delta$ states of $^2[Mn(O)(H_8Cz)]^+$ (left) and high-lying occupied MOs (right).

geometry optimizations and associated energies were successfully calculated for the doublet and quartet states of $[Mn(O)(H_8Cz)]^+$, wherein all of the peripheral substituents on the Cz ring were replaced with H atoms. There are three low-lying doublet spin states: the lowest two are the $^2A'$ $[\delta^2(a')^1(a'')^2]$ and $^2A''$ $[\delta^2(a')^2(a'')^1]$ states, both representing a $[Mn^V(O)(H_8Cz^{+\bullet})]$ configuration, while the third is the $^2\Delta$ $[\delta^1(a')^2(a'')^2]$ state, representing a $[Mn^{VI}(O)(H_8Cz)]^+$ configuration. The $^2A''$ state was found to be the ground state and is well-separated from the $^2A'$ and $^2\Delta$ states, which lie 16.2 and 37.4 kcal mol^{-1} higher in energy, respectively. These results are in good agreement with the conclusion based on the CV, spectroelectrochemistry, and EPR data that the locus of oxidation upon conversion of **2** to $\mathbf{2}^+$ is the π system of the Cz ring and not the Mn ion.

The optimized geometry and high-lying occupied molecular orbitals (MOs) for the $^2A''$ ground state are shown in Figure 2. The structural parameters from the optimized geometry for $^2[Mn^V(O)(H_8Cz^{+\bullet})]$ reveal Mn−N and Mn−O bond lengths that compare well to the distances obtained for **2** from EXAFS $[(Mn-N_{pyrrole})_{ave}$ = 1.88(4) Å, Mn−O = 1.56(2) Å].[9b] The a″ orbital in Figure 2 is the singly occupied MO and is analogous to the a_{1u} orbital in porphyrins. This orbital has almost no spin density on either the *meso*- or pyrrole N atoms, which agrees with the lack of hyperfine splitting in the EPR spectrum. Metalloporphyrin π-cation radicals $[M(por^{+\bullet})]$ typically exhibit a singly occupied a_{2u} orbital analogous to a′ in Figure 2, but the electron-withdrawing *meso*-N atoms of the Cz ring likely stabilize this orbital and lower it below the a″ orbital.[14] DFT calculations give d(Mn−O) = 1.542 Å for $^2[Mn^V(O)(H_8Cz^{+\bullet})]$ which is slightly shorter than either the DFT-derived (1.549 Å)[9d] or EXAFS-derived distance for **2**. Similarly, the DFT-derived ν(Mn−O) of 990 cm^{-1} for $^2[Mn^V(O)(H_8Cz^{+\bullet})]$ is higher than ν(Mn−O) = 975 cm^{-1} for $^1[Mn^V(O)(H_8Cz)]$. This predicted increase in ν(Mn−O) for the π-cation radical is opposite to that seen for Cpd-I [ν(Fe−O) = 801−835 cm^{-1}] versus Cpd-II [ν(Fe−O) = 843 cm^{-1}] in synthetic porphyrin analogues.[15] However, the former Cpd-I is an a_{2u} ferryl π-cation radical. A better comparison with $\mathbf{2}^+$/**2** is $[V(O)(por^{+\bullet})]$ with a_{1u} symmetry [, υ(V−O)= 1002 cm^{-1}) versus $[V(O)(por)]$ (υ(V−O)= 987 cm^{-1}).[16]

The facile generation and relative stability of $\mathbf{2}^+$ allowed us to investigate its reactivity toward OAT. Complex $\mathbf{2}^+$ reacted rapidly with 1 equiv of PPh_3 at 25 °C to produce $OPPh_3$ in good yield (71%) (Scheme 2). When this reaction was monitored by UV−vis spectroscopy, isosbestic conversion of $\mathbf{2}^+$ to a new spectrum with λ_{max} = 440, 678(sh), and 722 nm was observed (Figure S4), which matches that for $[(TBP_8Cz)Mn^{IV}]^+$.[17] The UV−vis data show that a smooth two-electron OAT process occurred following addition of PPh_3 to $\mathbf{2}^+$. The oxo source was identified as $\mathbf{2}^+$ by ^{18}O isotopic enrichment of the terminal oxo group. Reaction of **$\mathbf{2}^+$-^{18}O** with PPh_3 gave $^{18}OPPh_3$ (55% incorporation by GC−MS).

dx.doi.org/10.1021/ja2066237 |J. Am. Chem. Soc. 2011, 133, 15874–15877

Scheme 2. OAT Reactions

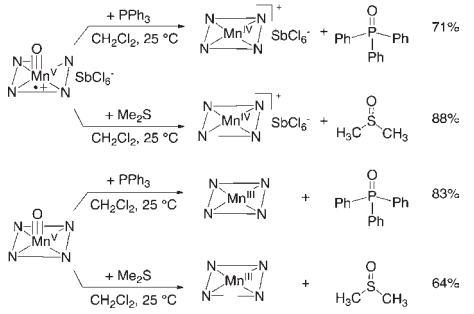

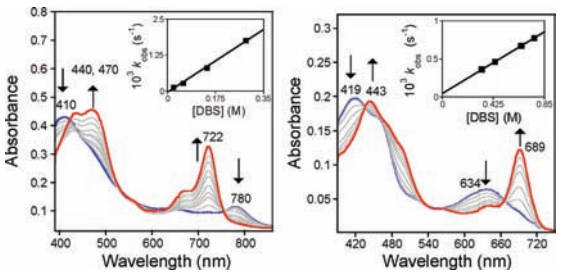

Figure 3. Time-resolved UV−vis spectra of the reactions between (left) $\mathbf{2}^+$ (9.5 μM) and DBS (72 mM) at 25 °C to give $[(TBP_8Cz)Mn^{IV}]^+$ (440, 722 nm) and (right) **2** (3.2 μM) and DBS (0.4 M) at 35 °C to give **1** (443, 689 nm) in toluene. Insets: second-order plots.

Complex $\mathbf{2}^+$ was also found to be competent to oxidize thermodynamically more challenging thioether substrates to their corresponding sulfoxides. Addition of excess dimethyl sulfide (DMS) to a solution of $\mathbf{2}^+$ in CH_2Cl_2 resulted in the production of dimethyl sulfoxide (DMSO) (88% by GC) (Scheme 2). UV−vis spectroscopy revealed isosbestic conversion of $\mathbf{2}^+$ to $[(TBP_8Cz)Mn^{IV}]^+$, as seen for the reaction with PPh_3. Analysis of the DMS reaction mixture by EPR spectroscopy upon completion showed an intense high-spin Mn^{IV} ($S = {}^3/_2$) signal with $g = 4.68$, 3.28, and 1.94 and well-resolved ^{55}Mn hyperfine splitting (Figure S8). The EPR data confirm that Mn^{IV} was produced following OAT from $\mathbf{2}^+$ to thioether substrates.

A previous study showed that the neutral Mn^V−oxo complex **2** is capable of OAT to PPh_3, generating $OPPh_3$ in good yield (83%) along with Mn^{III} complex **1**. Qualitative UV−vis data also suggested that DMS can reduce **2** to **1**.[9a] Here we confirmed that DMSO (64%) is produced in this reaction. The kinetics of OAT for $\mathbf{2}^+$ and **2** with DMS under pseudo-first-order conditions was monitored by UV−vis spectroscopy in CH_2Cl_2 (Figures S6 and S7). Both complexes exhibited good pseudo-first-order kinetics, and a linear dependence of the observed rate constants (k_{obs}) on [DMS] gave the second-order rate constants $k(\mathbf{2}^+) = 0.25 \pm 0.05\ M^{-1}\ s^{-1}$ and $k(\mathbf{2}) = (2.0 \pm 0.2) \times 10^{-3}\ M^{-1}\ s^{-1}$, indicating a large rate enhancement for $\mathbf{2}^+$ over **2** in OAT.

The temperature dependence of $k(\mathbf{2}^+)$ and $k(\mathbf{2})$ was measured in toluene with the less volatile *n*-Bu_2S (DBS) in place of DMS as the substrate. Good isosbestic behavior and pseudo-first-order kinetics were also observed for this substrate (Figure 3). Plots of $\ln(k/T)$ versus $1/T$ (Figure S11) were linear for both complexes and yielded the activation parameters given in Table 1. The enthalpy of activation for **2**, $\Delta H^{\ddagger} = 16 \pm 1$ kcal mol^{-1}, decreased significantly upon one-electron oxidation, with $\Delta\Delta H^{\ddagger} = -9$ kcal mol^{-1} for $\mathbf{2}^+$ versus **2**. Large negative $\Delta S^{\ddagger}$ values were found for both complexes, indicating that the two oxidants operate through

Table 1. Kinetic Parameters for OAT Reactions with DBS

	2	$\mathbf{2}^+$
k^a	3.8×10^{-4} [b]	$(6.2 \pm 0.2) \times 10^{-3}$
$\Delta H^{\ddagger}$ [c]	16 ± 1 [12.3][d]	7.0 ± 0.8 [7.1][d]
$\Delta S^{\ddagger}$ [e]	-20 ± 4	-45 ± 3
$\Delta G^{\ddagger}$ (298 K)[c]	22 ± 2 [23.8][d]	20 ± 2 [17.6][d]

[a] Values in $M^{-1}\ s^{-1}$ at 298 K. [b] Extrapolated from the $\ln(k/T)$ vs $1/T$ plot. [c] Values in kcal mol^{-1}. [d] DFT-calculated value for the reaction with DMS. [e] Values in cal K^{-1} mol^{-1}.

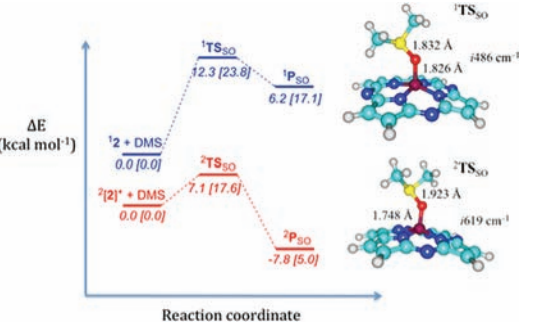

Figure 4. Potential energy profiles for the OAT reactions of **2** and $\mathbf{2}^+$ with DMS. Energies (ΔE + ZPE + E_{solv}) are given, with free energies in brackets. The optimized transition-state geometries are shown at the right.

similar bimolecular OAT mechanisms. The decrease in $\Delta H^{\ddagger}$ for $\mathbf{2}^+$ is somewhat attenuated by its more negative $\Delta S^{\ddagger}$ value,[18] as reflected in the smaller difference (~2 kcal mol^{-1}) in the $\Delta G^{\ddagger}$ values for $\mathbf{2}^+$ and **2** at 298 K.

DFT calculations were employed to compare the mechanisms of sulfoxidation for $\mathbf{2}^+$ and **2**. DMS was used in place of DBS as the substrate to facilitate the calculations. The potential energy profiles (Figure 4) reveal single transition states ($\mathbf{TS}_{SO}$) proceeding to sulfoxide products ($\mathbf{P}_{SO}$) for both oxidants. These profiles indicate that **2** and $\mathbf{2}^+$ proceed through the same concerted bimolecular OAT mechanism. This mechanistic conclusion agrees well with the experimentally derived $\Delta S^{\ddagger}$ values for $\mathbf{2}^+$ and **2** and the results of previous sulfoxidation studies.[19]

The DFT-derived $\Delta H^{\ddagger}$ value (ΔE + ZPE + E_{solv}) for $\mathbf{2}^+$ is significantly lower than that for **2**, in good agreement with the trend seen experimentally. This large difference in activation enthalpies is unlikely to arise from changes in Mn−O bond strength for $\mathbf{2}^+$ vs **2**, given that our DFT calculations predict relatively minor increases in bond distance and ν(Mn−O), which might be expected to *increase* $\Delta H^{\ddagger}$ for OAT with $\mathbf{2}^+$.[20] However, both the calculated electron affinities (see the SI) and the experimentally derived reduction potentials for $\mathbf{2}^+$ relative to **2** point to a much higher electrophilicity for $\mathbf{2}^+$, and we suggest that the $\Delta H^{\ddagger}$ for OAT is dominated by the much greater *electrophilicity* of the oxidant in this case.[21] Few systematic studies are available that have similarly compared OAT reactivities for closely related metal−oxo species differing by only one oxidation level. Interestingly, however, Brown and co-workers reached similar conclusions regarding the impact of electrophilicity on OAT for two $Re^V(O)$ complexes differing by only one unit of charge.[22] Similarly, Mayer also highlighted the importance of electrophilicity in explaining the reactivity of a Re(dioxo) complex.[23]

dx.doi.org/10.1021/ja2066237 |J. Am. Chem. Soc. 2011, 133, 15874–15877

In conclusion, we have generated a $Mn^{V}(O)$ π-cation radical complex and shown that it is a more reactive oxidant for OAT reactions than its one-electron-reduced analogue. Our experimental data and theoretical calculations are in excellent agreement and point to a concerted OAT mechanism for both cationic and neutral oxidants. A recent study of $Mn^{V}(O)$ corroles and OAT to sulfides invoked a disproportionation mechanism to give a more reactive $Mn^{VI}(O)$(corrole) as the primary oxidant, although no direct evidence for this complex was presented.[24,25] While we found no evidence for the Mn^{VI} oxidation state, our results indicate that the isoelectronic species $Mn^{V}(O)(Cz^{+\bullet})$ is indeed a reactive oxidant. In relating our findings to the relative reactivity of Cpd-I versus Cpd-II in heme enzymes and models, we suggest that a simple advantage in electrophilicity for Cpd-I may play a significant role in determining the greater reactivity usually associated with this species. Further work is necessary to determine the relative reactivity of **2** versus $\mathbf{2}^{+}$ in other oxidative transformations of biological and catalytic relevance.

■ ASSOCIATED CONTENT

Supporting Information. Experimental procedures, Figures S1−S15, and computational details. This material is available free of charge via the Internet at http://pubs.acs.org.

■ AUTHOR INFORMATION

Corresponding Author
sam.devisser@manchester.ac.uk; dpg@jhu.edu

■ ACKNOWLEDGMENT

This work was supported by the NSF (CHE0909587) to D.P.G. and the Harry and Cleio Greer Fellowship to K.A.P. S.P.d.V. thanks the National Service of Computational Chemistry Software for CPU time and the University of Manchester for a travel grant. We thank R. Czernuszewicz for useful discussions.

■ REFERENCES

(1) (a) Sono, M.; Roach, M. P.; Coulter, E. D.; Dawson, J. H. *Chem. Rev.* **1996**, *96*, 2841. (b) Groves, J. T. *Proc. Natl. Acad. Sci. U.S.A.* **2003**, *100*, 3569. (c) Denisov, I. G.; Makris, T. M.; Sligar, S. G.; Schlichting, I. *Chem. Rev.* **2005**, *105*, 2253. (d) *Cytochrome P450: Structure, Mechanism and Biochemistry*, 3rd ed.; Ortiz de Montellano, P. R., Ed.; Kluwer Academic/Plenum Publishers: New York, 2004. (e) Rittle, J.; Green, M. T. *Science* **2010**, *330*, 933. (f) Dunford, H. B. *Heme Peroxidases*; Wiley-VCH: New York, 1999.

(2) (a) Bruijnincx, P. C.; van Koten, G.; Klein Gebbink, R. J. *Chem. Soc. Rev.* **2008**, *37*, 2716. (b) Krebs, C.; Galonić Fujimori, D.; Walsh, C. T.; Bollinger, J. M., Jr. *Acc. Chem. Res.* **2007**, *40*, 484. (c) Que, L., Jr. *Acc. Chem. Res.* **2007**, *40*, 493. (d) Solomon, E. I.; Brunold, T. C.; Davis, M. I.; Kemsley, J. N.; Lee, S. K.; Lehnert, N.; Neese, F.; Skulan, A. J.; Yang, Y. S.; Zhou, J. *Chem. Rev.* **2000**, *100*, 235. (e) Ryle, M. J.; Hausinger, R. P. *Curr. Opin. Chem. Biol.* **2002**, *6*, 193.

(3) Nam, W. *Acc. Chem. Res.* **2007**, *40*, 522.

(4) (a) McEvoy, J. P.; Brudvig, G. W. *Chem. Rev.* **2006**, *106*, 4455. (b) Betley, T. A.; Wu, Q.; Van Voorhis, T.; Nocera, D. G. *Inorg. Chem.* **2008**, *47*, 1849. (c) Umena, Y.; Kawakami, K.; Shen, J. R.; Kamiya, N. *Nature* **2011**, *473*, 55.

(5) For examples, see: (a) Parsell, T. H.; Yang, M. Y.; Borovik, A. S. *J. Am. Chem. Soc.* **2009**, *131*, 2762. (b) Yin, G. C.; Danby, A. M.; Kitko, D.; Carter, J. D.; Scheper, W. M.; Busch, D. H. *J. Am. Chem. Soc.* **2007**, *129*, 1512. (c) Arunkumar, C.; Lee, Y. M.; Lee, J. Y.; Fukuzumi, S.; Nam, W. *Chem.—Eur. J.* **2009**, *15*, 11482. (d) Kurahashi, T.; Kikuchi, A.; Shiro, Y.; Hada, M.; Fujii, H. *Inorg. Chem.* **2010**, *49*, 6664. (e) Sastri, C. V.; Lee, J.; Oh, K.; Lee, Y. J.; Lee, J.; Jackson, T. A.; Ray, K.; Hirao, H.; Shin, W.; Halfen, J. A.; Kim, J.; Que, L., Jr.; Shaik, S.; Nam, W. *Proc. Natl. Acad. Sci. U.S.A.* **2007**, *104*, 19181. (f) Wang, D.; Zhang, M.; Buhlmann, P.; Que, L., Jr. *J. Am. Chem. Soc.* **2010**, *132*, 7638. (g) Miller, C. G.; Gordon-Wylie, S. W.; Horwitz, C. P.; Strazisar, S. A.; Peraino, D. K.; Clark, G. R.; Weintraub, S. T.; Collins, T. J. *J. Am. Chem. Soc.* **1998**, *120*, 11540.

(6) (a) Groves, J. T.; Lee, J.; Marla, S. S. *J. Am. Chem. Soc.* **1997**, *119*, 6269. (b) Song, W. J.; Seo, M. S.; George, S. D.; Ohta, T.; Song, R.; Kang, M. J.; Tosha, T.; Kitagawa, T.; Solomon, E. I.; Nam, W. *J. Am. Chem. Soc.* **2007**, *129*, 1268. (c) Nam, W.; Kim, I.; Lim, M. H.; Choi, H. J.; Lee, J. S.; Jang, H. G. *Chem.—Eur. J.* **2002**, *8*, 2067. (d) Jin, N.; Ibrahim, M.; Spiro, T. G.; Groves, J. T. *J. Am. Chem. Soc.* **2007**, *129*, 12416.

(7) (a) Altun, A.; Shaik, S.; Thiel, W. *J. Am. Chem. Soc.* **2007**, *129*, 8978. (b) Tahsini, L.; Bagherzadeh, M.; Nam, W.; de Visser, S. P. *Inorg. Chem.* **2009**, *48*, 6661. (c) Latifi, R.; Tahsini, L.; Karamzadeh, B.; Safari, N.; Nam, W.; de Visser, S. P. *Arch. Biochem. Biophys.* **2011**, *507*, 4. (d) *Metal−Oxo and Metal−Peroxo Species in Catalytic Oxidations*; Meunier, B., Ed.; Springer: Berlin, 2000. (e) McLain, J.; Lee, J.; Groves, J. T. In *Biomimetic Oxidations*; Meunier, B., Ed.; Imperial College Press: London, 1999; pp 91−170.

(8) For a related study, see: Pan, Z.; Wang, Q.; Sheng, X.; Horner, J. H.; Newcomb, M. *J. Am. Chem. Soc.* **2009**, *131*, 2621.

(9) (a) Mandimutsira, B. S.; Ramdhanie, B.; Todd, R. C.; Wang, H.; Zareba, A. A.; Czernuszewicz, R. S.; Goldberg, D. P. *J. Am. Chem. Soc.* **2002**, *124*, 15170. (b) Lansky, D. E.; Mandimutsira, B.; Ramdhanie, B.; Clausen, M.; Penner-Hahn, J.; Zvyagin, S. A.; Telser, J.; Krzystek, J.; Zhan, R.; Ou, Z.; Kadish, K. M.; Zakharov, L.; Rheingold, A. L.; Goldberg, D. P. *Inorg. Chem.* **2005**, *44*, 4485. (c) Lansky, D. E.; Goldberg, D. P. *Inorg. Chem.* **2006**, *45*, 5119. (d) Prokop, K. A.; de Visser, S. P.; Goldberg, D. P. *Angew. Chem., Int. Ed.* **2010**, *49*, 5091.

(10) Connelly, N. G.; Geiger, W. E. *Chem. Rev.* **1996**, *96*, 877.

(11) (a) Simkhovich, L.; Mahammed, A.; Goldberg, I.; Gross, Z. *Chem.—Eur. J.* **2001**, *7*, 1041. (b) Goldberg, I.; Meier-Callahan, A. E.; Di Bilio, A. J.; Simkhovich, L.; Mahammed, A.; Gray, H. B.; Gross, Z. *Inorg. Chem.* **2001**, *40*, 6788.

(12) Gross, Z. *J. Biol. Inorg. Chem.* **2001**, *6*, 733.

(13) (a) de Visser, S. P. *J. Am. Chem. Soc.* **2010**, *132*, 1087. (b) Kumar, D.; Karamzadeh, B.; Sastry, G. N.; de Visser, S. P. *J. Am. Chem. Soc.* **2010**, *132*, 7656.

(14) (a) Ghosh, A.; Wondimagegn, T.; Parusel, A. B. J. *J. Am. Chem. Soc.* **2000**, *122*, 5100. (b) Gross, Z.; Barzilay, C. *Angew. Chem., Int. Ed. Engl.* **1992**, *31*, 1615. (c) Barzilay, C. M.; Sibilia, S. A.; Spiro, T. G.; Gross, Z. *Chem.—Eur. J.* **1995**, *1*, 222.

(15) Czarnecki, K.; Nimri, S.; Gross, Z.; Proniewicz, L. M.; Kincaid, J. R. *J. Am. Chem. Soc.* **1996**, *118*, 2929.

(16) Macor, K. A.; Czernuszewicz, R. S.; Spiro, T. G. *Inorg. Chem.* **1990**, *29*, 1996.

(17) Fukuzumi, S.; Kotani, H.; Prokop, K. A.; Goldberg, D. P. *J. Am. Chem. Soc.* **2011**, *133*, 1859.

(18) The origin of the large magnitude of $\Delta S^{\ddagger}$ for $\mathbf{2}^{+}$ is unknown, but for a comparable value, see: Costas, M.; Garcia-Bosch, I.; Company, A.; Cady, C. W.; Styring, S.; Browne, W. R.; Ribas, X. *Angew. Chem., Int. Ed.* **2011**, *50*, 5647.

(19) Kumar, D.; Sastry, G. N.; de Visser, S. P. *Chem.—Eur. J.* **2011**, *17*, 6196.

(20) (a) Holm, R. H.; Tucci, G. C.; Donahue, J. P. *Inorg. Chem.* **1998**, *37*, 1602. (b) Shaik, S.; Kang, Y.; Chen, H.; Jeong, Y. J.; Lai, W.; Bae, E. H.; Nam, W. *Chem.—Eur. J.* **2009**, *15*, 10039.

(21) It should be noted that the kinetics of OAT and the driving force are not easily correlated. See: Abu-Omar, M. M.; Appelman, E. H.; Espenson, J. H. *Inorg. Chem.* **1996**, *35*, 7751.

(22) Seymore, S. B.; Brown, S. N. *Inorg. Chem.* **2000**, *39*, 325.

(23) DuMez, D. D.; Mayer, J. M. *Inorg. Chem.* **1998**, *37*, 445.

(24) Kumar, A.; Goldberg, I.; Botoshansky, M.; Buchman, Y.; Gross, Z. *J. Am. Chem. Soc.* **2010**, *132*, 15233.

(25) For the generation of a (nitrido)manganese(VI) corrole, see: Golubkov, G.; Gross, Z. *J. Am. Chem. Soc.* **2005**, *127*, 3258.